AIAA JOURNAL
Vol. 33, No. 12, December 1995

Application of the Finite Element Method to Postbuckling Analysis of Laminated Plates

Le-Chung Shiau* and Teng-Yuan Wu†
National Cheng Kung University, Tainan, Taiwan 70101, Republic of China

Based on the von Kármán large deformation assumptions, a 72-degree-of-freedom high-precision higher order triangular plate element using a simplified higher order shear deformation plate theory is developed for the analysis of postbuckling behavior of a composite laminated plate subjected to edge shortening or in-plane compressive loading. By examining the local minimum of total potential energy of each mode, a clear picture of buckled pattern change is presented. Results show that the buckled pattern change may occur for plates with certain material properties and boundary conditions. The important transverse shear effect on the buckled pattern change is also presented. It shows that the buckling mode will shift from first to second mode shortly after buckling occurs if the transverse shear deformation is included.

Nomenclature

D = bending rigidity
E_1, E_2 = Young's modulus referred to principal material direction
G_{ij} = shear modulus
$[H]$ = Hessian matrix of plate system
h = plate thickness
$[K_l]$ = linear stiffness matrix of plate
$[k_l]$ = linear element stiffness matrix
$[K_t]$ = tangent stiffness matrix
L = width of plate
N_x = in-plane loading induced by edge shortening
$[N_1]$ = first-order nonlinear stiffness matrix of plate
$[N_2]$ = second-order nonlinear stiffness matrix of plate
$[n_1]$ = first-order nonlinear element stiffness matrix
$[n_2]$ = second-order nonlinear element stiffness matrix
$\{P\}$ = consistent load vector
p = in-plane loading
p_{cr} = critical buckling load
$\{Q\}$ = total degree of freedom
$\bar{Q}_{ij}$ = transformed reduced stiffness
$\{q\}$ = element degree of freedom
U = total strain energy of the laminate
U_2 = strain energy of quadratic form
U_3 = strain energy of cubic form
U_4 = strain energy of quartic form
u, v, w = displacement fields in the x, y, z directions
W_c = work done by conservative force
x, y, z = global coordinates system
ϵ_{ij} = strain components
ν_{ij} = Poisson modulus of lamina
ξ, η = local coordinates system
π = total potential energy
σ_{ij} = stress components

Subscripts

0 = uniform in-plane displacement
$'$ = derivative with respect to the variable

Superscripts

b = deflection due to bending deformation
s = deflection due to shear deformation
T = transpose of a vector or matrix

Received June 20, 1994; revision received Feb. 17, 1995; accepted for publication Feb. 20, 1995.

*Professor, Institute of Aeronautics and Astronautics.
†Graduate Student, Institute of Aeronautics and Astronautics.

Introduction

IT is known that a plate is capable of carrying a much increased load after buckling without failure. Therefore, it is necessary to consider the behavior of the plate after buckling, i.e., the postbuckling behavior, to fully utilize the strength of the plate and to reduce weight of plate material. A precise analysis of postbuckling behavior is quite difficult due to the use of the nonlinear plate theory and to the buckled pattern changes that occur in the buckled state. The buckled pattern change, which is often encountered in experiments, occurs when the energy stored in the plate is sufficient to carry the plate from one buckled pattern to another. In most postbuckling analyses, the buckled pattern of the plate is assumed to remain unchanged. This is only a reasonable assumption in the immediate vicinity of the buckling load. To obtain a detailed analysis of plate response over a wide postbuckling load range, changes in buckling pattern must be taken into consideration.

An early discussion of buckled pattern change was presented by Stein[1] for a three-bar-column model subjected to axial compressive load. In his subsequent paper,[2] he considered buckled pattern change for the postbuckling analysis of isotropic plates with various aspect ratios. He concluded that the intersection of the load-shortening curves indicates possible changes in buckled pattern. The postbuckling behavior of composite plates has been discussed by various investigators.[3–9] Among these studies, the postbuckling behavior with no buckled pattern change assumption usually concerns the relation of in-plane compressive force vs transverse deflection or in-plane compressive force vs buckled bending stress. Chia[10] in 1988 reviewed geometrically nonlinear behavior of composite plates and pointed out that the buckled pattern change may occur if p/p_{cr} is greater than 3.0. Recently, Shin et al.[11] proposed a different approach to examine the buckled pattern change. He compared the magnitude of the total potential energy of each buckling mode. The mode which has the minimum value of the total potential energy is assumed to represent the actual buckled pattern. However, he only checked the first variation of the total potential energy, which may not necessarily give the local minimum of the total potential energy.

Based on von Kármán large deformation assumptions, a 72-degree-of-freedom (DOF) high-precision triangular plate element developed in Ref. 12 is extended to study the postbuckling behavior of a composite laminated plate subjected to edge shortening or in-plane compressive load. This plate element was developed based on a simplified higher order shear deformation plate theory that satisfies zero transverse shear stress conditions on the free boundary planes and does not require a shear correction factor. The element presents no shear locking problem[12] due to the assumption that the total transverse displacement of the plate is expressed as the sum of

the displacement due to bending and that due to shear deformation. The results obtained by this element for free vibration analysis of various composite laminates[12] are in excellent agreement with those obtained by using three-dimensional elasticity and other solutions.

Formulations

Simplified Higher Order Plate Theory

Consider a laminated plate as shown in Fig. 1. The total transverse displacement of the plate is assumed to be the sum of the displacement due to bending alone and that due to shear deformation alone,

$$w(x, y, z) = w^b(x, y) + w^s(x, y) \tag{1}$$

where w^b and w^s denote the displacements of the midplane due to bending and shear deformation, respectively.

The in-plane displacements can also be expressed as the sum of the displacements due to bending and shear deformation,

$$u(x, y, z) = u_0(x, y) + u^b(x, y, z) + u^s(x, y, z) \tag{2a}$$

$$v(x, y, z) = v_0(x, y) + v^b(x, y, z) + v^s(x, y, z) \tag{2b}$$

in which u_0 and v_0 are the uniform in-plane displacement components of the plate. The in-plane displacements u^b and v^b due to bending follow the Kirchhoff hypotheses and vary linearly through the thickness. The in-plane displacements u^s and v^s due to shear deformation are assumed to vary cubically through the thickness so that the zero transverse shear strain conditions at the free surfaces are satisfied, and the transverse shear stresses are varied parabolically through the plate thickness. Based on these assumptions, the in-plane displacements may also be expressed in terms of w^b and w^s as

$$u(x, y, z) = u_0 - z\frac{\partial w^b}{\partial x} - \frac{4z^3}{3h^2}\frac{\partial w^s}{\partial x} \tag{3a}$$

$$v(x, y, z) = v_0 - z\frac{\partial w^b}{\partial y} - \frac{4z^3}{3h^2}\frac{\partial w^s}{\partial y} \tag{3b}$$

where h is the plate thickness.

Adopting the von Kármán large deflection assumptions, the strain-displacement relations can then be determined from those displacement functions as

$$\epsilon_1 \equiv \epsilon_{xx} = \frac{\partial u_0}{\partial x} - z\frac{\partial^2 w^b}{\partial x^2} - \frac{4z^3}{3h^2}\frac{\partial^2 w^s}{\partial x^2} + \frac{1}{2}\left(\frac{\partial w}{\partial x}\right)^2$$

$$\epsilon_2 \equiv \epsilon_{yy} = \frac{\partial v_0}{\partial y} - z\frac{\partial^2 w^b}{\partial y^2} - \frac{4z^3}{3h^2}\frac{\partial^2 w^s}{\partial y^2} + \frac{1}{2}\left(\frac{\partial w}{\partial y}\right)^2$$

$$\epsilon_3 \equiv \epsilon_{zz} = 0$$

$$\epsilon_6 \equiv 2\epsilon_{xy} = \frac{\partial u_0}{\partial y} + \frac{\partial v_0}{\partial x} - 2z\frac{\partial^2 w^b}{\partial x \partial y} - \frac{8z^3}{3h^2}\frac{\partial^2 w^s}{\partial x \partial y} + \left(\frac{\partial w}{\partial x}\right)\left(\frac{\partial w}{\partial y}\right) \tag{4}$$

$$\epsilon_4 \equiv 2\epsilon_{yz} = \left(1 - \frac{4z^2}{h^2}\right)\frac{\partial w^s}{\partial y}$$

$$\epsilon_5 \equiv 2\epsilon_{xz} = \left(1 - \frac{4z^2}{h^2}\right)\frac{\partial w^s}{\partial x}$$

The total strain energy of the laminated plate is

$$U = \frac{1}{2}\int_v \{\sigma\}^T\{\epsilon\}\,dv \tag{5}$$

where the stress vector $\{\sigma\}$ and strain vector $\{\epsilon\}$ are defined as

$$\{\sigma\}^T = \langle \sigma_1 \quad \sigma_2 \quad \sigma_4 \quad \sigma_5 \quad \sigma_6 \rangle \tag{6a}$$

$$\{\epsilon\}^T = \langle \epsilon_1 \quad \epsilon_2 \quad \epsilon_4 \quad \epsilon_5 \quad \epsilon_6 \rangle \tag{6b}$$

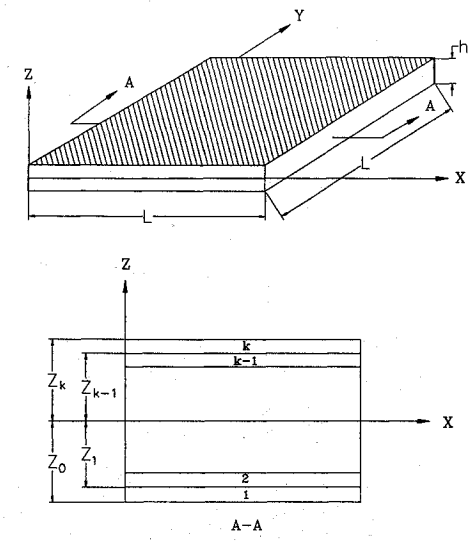

Fig. 1 Geometry of laminated plate.

For a composite laminated plate with n layers, the stress-strain relation of kth layer of the plate can be expressed in the plate coordinate system[13]

$$\{\sigma\}_k = [\bar{Q}]_k\{\epsilon\}_k \tag{7}$$

where $\bar{Q}_{ij}$ are the transformed reduced stiffnesses. By substituting Eqs. (4) and (7) into Eq. (5), the total strain energy of a composite laminated plate can be expressed as the sum of quadratic, cubic, and quartic displacement functions as

$$U = U_2 + U_3 + U_4 \tag{8}$$

where

$$U_2 = \frac{1}{2}\int_A (\{I\}^T[A]\{I\} + 2\{I\}^T[B]\{K\} + 2\{L\}^T[E]\{I\} + \{K\}^T[D]\{K\} + 2\{L\}^T[F]\{K\} + \{L\}^T[H]\{L\} + \{M\}^T[\bar{A}]\{M\} + 2\{N\}^T[\bar{D}]\{M\} + \{N\}^T[\bar{F}]\{N\})\,dx\,dy$$

$$U_3 = \frac{1}{2}\int_A (2\{J\}^T[A]\{I\} + 2\{J\}^T[B]\{K\} + 2\{J\}^T[E]\{L\})\,dx\,dy$$

$$U_4 = \frac{1}{2}\int_A \{J\}^T[A]\{J\}\,dx\,dy$$

and

$$\{I\} = \begin{Bmatrix} u_{0,x} \\ v_{0,y} \\ u_{0,y} + v_{0,x} \end{Bmatrix}, \quad \{K\} = \begin{Bmatrix} -w^b_{,xx} \\ -w^b_{,yy} \\ -2w^b_{,xy} \end{Bmatrix}, \quad \{L\} = \begin{Bmatrix} \frac{-4}{3h^2}w^s_{,xx} \\ \frac{-4}{3h^2}w^s_{,yy} \\ \frac{-8}{3h^2}w^s_{,xy} \end{Bmatrix}$$

$$\{M\} = \begin{Bmatrix} w^s_{,y} \\ w^s_{,x} \end{Bmatrix}, \quad \{N\} = \begin{Bmatrix} \frac{-4}{h^2}w^s_{,y} \\ \frac{-4}{h^2}w^s_{,x} \end{Bmatrix}, \quad \{J\} = \begin{Bmatrix} \frac{1}{2}(w_{,x})^2 \\ \frac{1}{2}(w_{,y})^2 \\ w_{,x}w_{,y} \end{Bmatrix}$$

$$(A_{ij}, B_{ij}, D_{ij}, E_{ij}, F_{ij}, H_{ij}) = \sum_{k=1}^{n}\int_{z_{k-1}}^{z_k} \bar{Q}_{ij}(1, z, z^2, z^4, z^6)\,dz \qquad (i, j = 1, 2, 6)$$

$$(\bar{A}_{ij}, \bar{D}_{ij}, \bar{F}_{ij}) = \sum_{k=1}^{n}\int_{z_{k-1}}^{z_k} \bar{Q}_{ij}(1, z^2, z^4)\,dz \qquad (i, j = 4, 5)$$

The work, due to the in-plane loading $p(x, y)$ integrating over the side of the element along which the load is applied, is given as

$$W_c = \int u(x, y)p(x, y)\,\mathrm{d}s \tag{9}$$

and the total potential energy of the laminate is then expressed as

$$\pi = U - W \tag{10}$$

The nonlinear equilibrium equation of the laminated plate can be derived by taking first variation of the total potential energy π of the plate as

$$\delta\pi = 0 \tag{11}$$

and the Hessian matrix of the laminated plate is obtained by taking second variation of the total potential energy of the plates as

$$[H] = \delta^2\pi \tag{12}$$

If the eigenvalues of the Hessian matrix are all positive, then the system is in a stable equilibrium state with its total potential energy in a local minimum stage.

Finite Element Formulation

Consider a 72-DOF triangular element with thickness h as shown in Fig. 2. The lateral displacement within this element is assumed to be the sum of the displacement due to bending and that due to shear deformation. For simplicity, the four displacement functions for the in-plane, bending, and shear deformation are assumed to have the same form. These displacement function for u, v, w^b, and w^s can be expressed in the local $\xi-\eta$ coordinate system as a polynomial to the complete fifth order of ξ and η, excluding the term $\xi^4\eta$. Omitting the term $\xi^4\eta$ is to ensure that the slope normal to the edge $\eta = 0$ varies cubically along ξ, so that the normal slope compatibility along this edge is satisfied:

$$u_0 = \sum_{i=1}^{20} \alpha_i \xi^{m_i} \eta^{n_i} \tag{13a}$$

$$v_0 = \sum_{i=1}^{20} \beta_i \xi^{m_i} \eta^{n_i} \tag{13b}$$

$$w^b = \sum_{i=1}^{20} \gamma_i \xi^{m_i} \eta^{n_i} \tag{13c}$$

$$w^s = \sum_{i=1}^{20} \zeta_i \xi^{m_i} \eta^{n_i} \tag{13d}$$

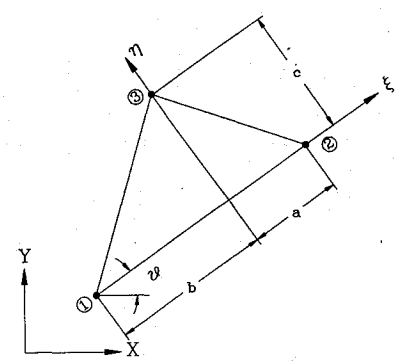

$$\text{DOF}: \begin{pmatrix} u & u_{,\xi} & u_{,\eta} & u_{,\xi\xi} & u_{,\xi\eta} & u_{,\eta\eta} \\ v & v_{,\xi} & v_{,\eta} & v_{,\xi\xi} & v_{,\xi\eta} & v_{,\eta\eta} \\ w^b & w^b_{,\xi} & w^b_{,\eta} & w^b_{,\xi\xi} & w^b_{,\xi\eta} & w^b_{,\eta\eta} \\ w^s & w^s_{,\xi} & w^s_{,\eta} & w^s_{,\xi\xi} & w^s_{,\xi\eta} & w^s_{,\eta\eta} \end{pmatrix}$$

Fig. 2 Coordinate system of triangular plate element.

where

$$m_i = (0,\ 1,\ 0,\ 2,\ 1,\ 0,\ 3,\ 2,\ 1,\ 0,\ 4,\ 3,\ 2,\ 1,\ 0,\ 5,\ 3,\ 2,\ 1,\ 0)$$

$$n_i = (0,\ 0,\ 1,\ 0,\ 1,\ 2,\ 0,\ 1,\ 2,\ 3,\ 0,\ 1,\ 2,\ 3,\ 4,\ 0,\ 2,\ 3,\ 4,\ 5)$$

and α_i, β_i, γ_i, ζ_i are constants to be determined by using conditions at nodal points. By following the procedure described in Ref. 14, the displacement functions with reference to the global coordinate can be expressed in terms of the element nodal displacement vector $\{q\}$. Substituting the displacement functions in Eqs. (13) into Eq. (8) and integrating over the plate element, the total strain energy of an element can be expressed as

$$U_e = \tfrac{1}{2}\{q\}^T[R]^T[T]^T\left[[k_l] + \tfrac{1}{3}[n_1] + \tfrac{1}{6}[n_2]\right][T][R]\{q\} \tag{14}$$

with

$$\{q\}^T = \left[\{q_u\}^T, \{q_v\}^T, \{q_{w^b}\}^T, \{q_{w^s}\}^T\right]$$

in which the matrices $[R]$ and $[T]$ are given in Ref. 14, matrices $[k_l]$, $[n_1]$, and $[n_2]$ are the linear, first-order, and second-order nonlinear stiffness matrices, respectively, and can be written in the following matrix form as

$$[k_l] = \begin{pmatrix} k_{l_{\alpha\alpha}} & k_{l_{\alpha\beta}} & k_{l_{\alpha\gamma}} & k_{l_{\alpha\zeta}} \\ k_{l_{\beta\alpha}} & k_{l_{\beta\beta}} & k_{l_{\beta\gamma}} & k_{l_{\beta\zeta}} \\ k_{l_{\gamma\alpha}} & k_{l_{\gamma\beta}} & k_{l_{\gamma\gamma}} & k_{l_{\gamma\zeta}} \\ k_{l_{\zeta\alpha}} & k_{l_{\zeta\beta}} & k_{l_{\zeta\gamma}} & k_{l_{\zeta\zeta}} \end{pmatrix} \tag{15a}$$

$$[n_1] = \begin{pmatrix} 0 & 0 & n_{1_{\alpha\gamma}} & n_{1_{\alpha\zeta}} \\ 0 & 0 & n_{1_{\beta\gamma}} & n_{1_{\beta\zeta}} \\ n_{1_{\gamma\alpha}} & n_{1_{\gamma\beta}} & n_{1_{\gamma\gamma}} & n_{1_{\gamma\zeta}} \\ n_{1_{\zeta\alpha}} & n_{1_{\zeta\beta}} & n_{1_{\zeta\gamma}} & n_{1_{\zeta\zeta}} \end{pmatrix} \tag{15b}$$

$$[n_2] = \begin{pmatrix} 0 & 0 & 0 & 0 \\ 0 & 0 & 0 & 0 \\ 0 & 0 & n_{2_{\gamma\gamma}} & n_{2_{\gamma\zeta}} \\ 0 & 0 & n_{2_{\zeta\gamma}} & n_{2_{\zeta\zeta}} \end{pmatrix} \tag{15c}$$

where

$$k_{l_{ij}} = \frac{\partial^2 U_2}{\partial q_i \partial q_j} \qquad n_{1_{ij}} = \frac{\partial^2 U_3}{\partial q_i \partial q_j} \qquad n_{2_{ij}} = \frac{\partial^2 U_4}{\partial q_i \partial q_j}$$

The details of the linear stiffness matrix $k_{l_{ij}}$ is given in Ref. 12 and the elements $n_{1_{ij}}$ and $n_{2_{ij}}$ are given explicitly in the Appendix.

By substituting Eqs. (13a) and (13b) into Eq. (9), and integrating along the loading edges of the plate element, the consistent load vector $\{p_f\}$ is obtained as

$$\{p_f\} = [R_2]^T[T_2]^T\{p_w\} \tag{16}$$

where the matrices $[R_2]$ and $[T_2]$ are submatrices of $[R]$ and $[T]$, and the column vector $\{p_w\}$ is expressed as

$$p_{w_i} = \int\int p\xi^{m_i}\eta^{n_i}\,\mathrm{d}\xi\,\mathrm{d}\eta$$

On assembling all element stiffness matrices and load vectors and applying kinematic boundary conditions, the statically nonlinear equilibrium equations may be written as

$$\left[[K_l] + \tfrac{1}{2}[N_1] + \tfrac{1}{3}[N_2]\right]\{Q\} = \{P\} \tag{17}$$

In the present study, the Newton–Raphson method is applied to solve this nonlinear system equations.

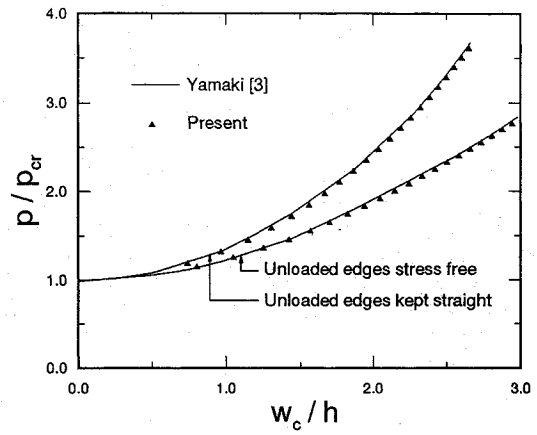

Fig. 3 Center deflection vs in-plane force of square isotropic plates subjected to edge shortening.

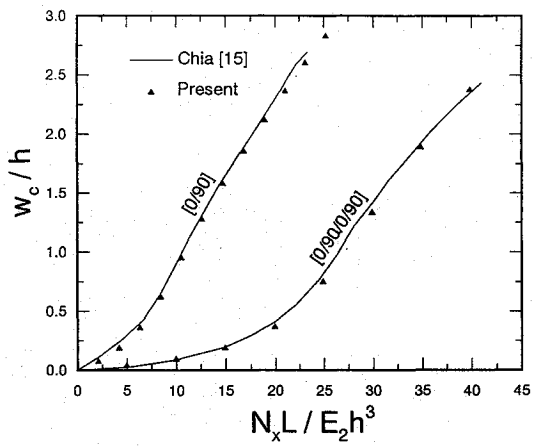

Fig. 4 Postbuckling behavior of square laminates with simply supported subjected to in-plane loading.

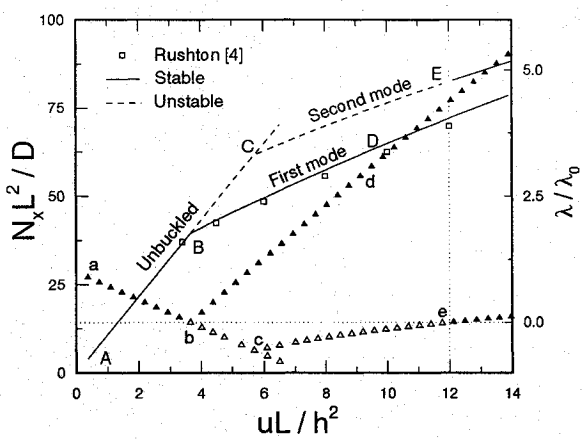

Fig. 5 Postbuckling behavior of square isotropic plate with unloaded edges, stress free: —, N_xL^2/D; △, λ/λ_0.

Numerical Results and Discussions

In the following analysis, the plate is modeled by using a 4 × 4 mesh with 32 elements. The material property for the laminates is $E_1/E_2 = 26.5$, $G_{12} = G_{13} = G_{23} = 1.184E_2$, and, $\nu_{12} = 0.21$. For the purposes of validation and comparison, the present computer code is first used to analyze a square, simply supported isotropic plate subjected to edge shortening which is identical to the one analyzed by Yamaki[3] using the analytical method. The results are presented in Fig. 3. It is seen that the results obtained by the present finite element method agree quite well with the analytical solution. Further, the postbuckling behaviors of two asymmetric cross-ply laminates studied by Chia[15] are also analyzed here, and the results are depicted in Fig. 4. The finite element results are in good agreement with those obtained by the series solution.

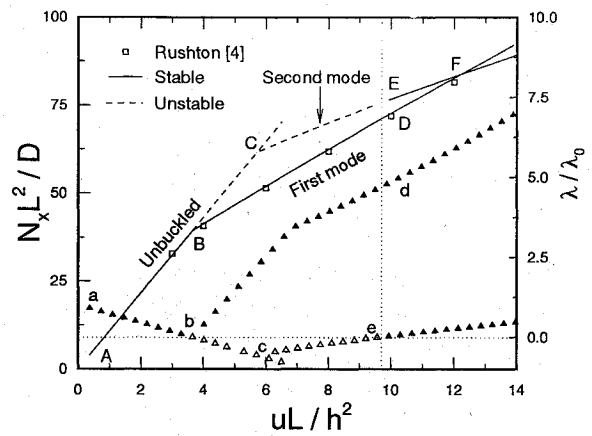

Fig. 6 Postbuckling behavior of square isotropic plate with unloaded edges kept straight: —, N_xL^2/D; △, λ/λ_0.

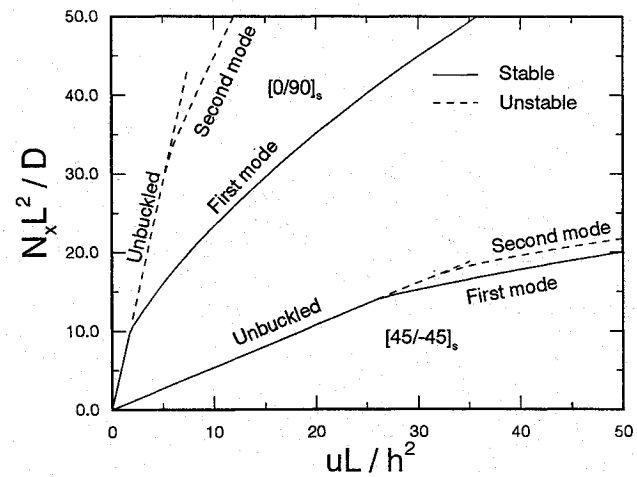

Fig. 7 Postbuckling behavior of square laminate with unloaded edges stress free.

Postbuckling of Square Plate Subjected to Edge Shortening

The results shown in Figs. 5 and 6 are the postbuckling behavior curves of a square isotropic plate with edge displacements vs in-plane forces and eigenvalues. Note that N_x is the in-plane force induced by the edge shortening in the x direction, λ is the minimum eigenvalue of the Hessian matrix, and λ_0 is the minimum eigenvalue of the Hessian matrix for a plate without edge shortening. The loaded edges of the plate are kept straight. The other two edges are stress free for the plate in Fig. 5 and kept straight for the plate in Fig. 6. The results from Ref. 4 are also shown in the figures as open rectangles for comparison purpose. The lines AB, BC, BD, and CE represent the load-shortening curves, and their corresponding curves ab, bc, bd, and ce are the lowest eigenvalues of the system in its equilibrium state. As the load is increased from zero, the plate remains flat until the load reaches point B. At this bifurcation point, the plate will buckle into first buckling mode due to the equilibrium state of the flat plate becoming unstable. It is also evident from the lines bc and bd that the lowest eigenvalue of the system for the unbuckled plate is negative and for the first buckling mode is positive. After buckling, the plate in Fig. 6 is stiffer than the plate in Fig. 5 due to the in-plane edge constraint of the plate in Fig. 6. Therefore, the slope of line BD in Fig. 6 is higher than that in Fig. 5. If the load is further increased beyond point F in Fig. 6, the plate will remain in the first buckling mode even though the load required to maintain the plate in the first mode is higher than that in the second mode. This is due to the fact that the system is in stable condition at this moment and the buckled pattern it will have is dependent on the previous deformed buckling shape. However, if there is enough external disturbed force, the buckling mode of the plate may shift from the first mode to the second, i.e., the total potential energy may jump from one local minimum point to another. Figure 7 shows the postbuckling behaviors of $[0/90]_s$ and $[\pm 45]_s$ laminates. It is seen that both laminates possess the same characteristics as those just stated for the

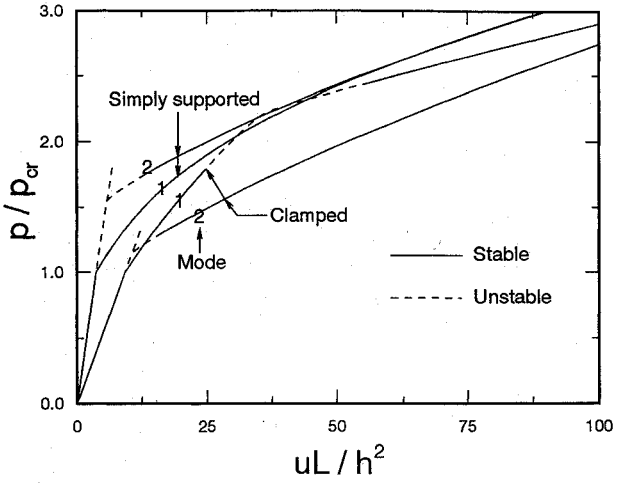

Fig. 8 Postbuckling behavior of square isotropic plate.

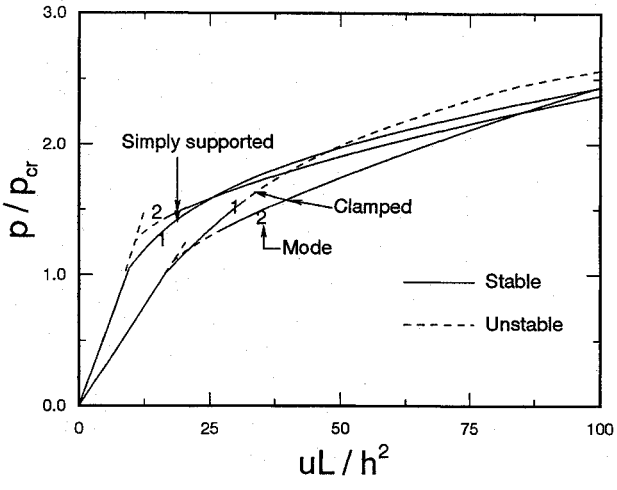

Fig. 9 Postbuckling behavior of square angle-ply $[45/-45]_s$ laminate.

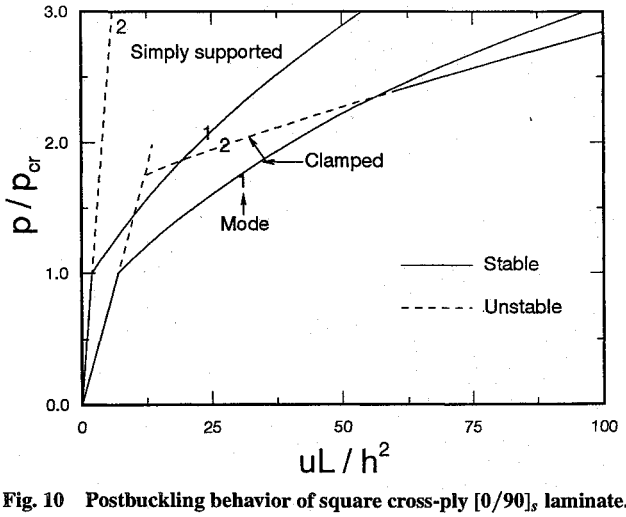

Fig. 10 Postbuckling behavior of square cross-ply $[0/90]_s$ laminate.

isotropic plate. From the trends of the eigenvalue curves (not shown in the figure), the second buckling mode of the $[0/90]_s$ laminate is always unstable.

Postbuckling of Square Laminate Subjected to In-Plane Loading

Usually, a square plate will buckle into, and remain in, the first buckling mode without a buckled pattern change if the load is gradually increased and there are no external disturbed forces. However, for some plates with certain material properties and boundary conditions, the first buckling mode may become unstable and the buckled pattern change may occur. Figures 8–10 show the postbuckling

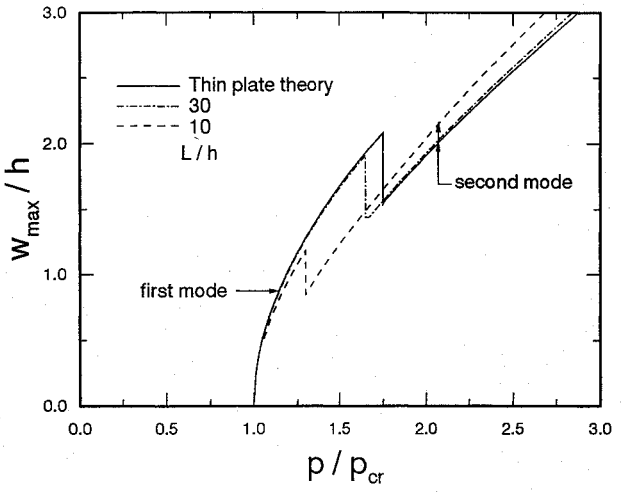

Fig. 11 Postbuckling behavior of square isotropic plate with clamped boundary condition.

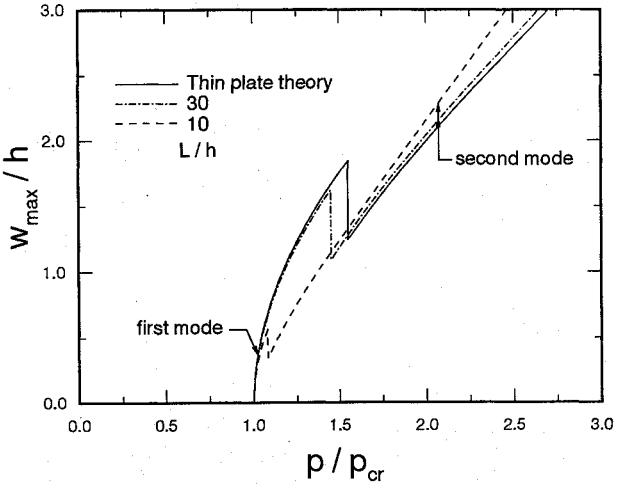

Fig. 12 Postbuckling behavior of square laminate $[45/-45]_s$ with clamped boundary condition.

behaviors of square plates subjected to uniaxial in-plane uniform load. The four edges are not necessarily kept straight. The plates with simply supported boundary conditions show the same postbuckling characteristics as those discussed in the preceding section for the edge shortening plates. But the isotropic and $[\pm 45]_s$ laminated plates with clamped edges display a different postbuckling behavior. When the in-plane load reaches the buckling load, the plates buckle into the first buckling mode. As the load is further increased to a certain value, the plate becomes unstable and the buckled pattern change occurs. The buckling mode of the plate is now shifted from the first mode to the second. The plate will remain in the second mode until the loading change causes the plate to become unstable again.

Transverse Shear Effect on Postbuckling Analysis of Square Plate

It is known that transverse shear has a significant effect on the mechanical behavior of a thick plate. Figures 11 and 12 show the effect of transverse shear on the buckled pattern change of the aforementioned isotropic and $[\pm 45]_s$ laminated plates with clamped edges. The results obtained using thin plate theory are also presented to indicate the extent of the transverse shear effect. It is seen that the buckled pattern change will occur earlier if the transverse shear deformation is included. The thicker the plate is, the earlier the buckled pattern change happens. For the $[\pm 45]_s$ laminate with $L/h = 10$, the buckled pattern is changed from the first mode to the second shortly after the buckling occurs. This may be attributed to the fact that the transverse shear deformation will reduce the lateral stiffness of the plate which, in turn, shifts the point of bifurcation to the left in the deflection-loading curve.

Conclusions

Based on von Kármán deformation assumptions, a 72-DOF high-precision triangular plate element using a simplified higher order shear deformation plate theory is developed for the analysis of postbuckling behavior of isotropic and composite laminated plates subjected to edge shortening or in-plane compressive load. By examining the local minimum of total potential energy of each mode, a clear picture of buckled pattern change may be seen. From the present results, the following conclusions can be made.

1) By checking the eigenvalues of the Hessian matrix of plate, the instability behavior of plates after buckling can be determined clearly.

2) The combination of loading type (edge shortening or uniform loading), material properties, and boundary conditions influences the trends and the occurrence of the buckled pattern change.

3) The buckled pattern change will occur earlier if the transverse shear deformation is considered. The thicker the plate is, the earlier the buckled pattern change happens.

Acknowledgment

The financial support from the National Science Council of the Republic of China through Grant NSC83-0405-E006-031 is highly appreciated.

Appendix: Elements in Nonlinear Stiffness Matrices

$$\left(n_{1_{\alpha\gamma}}\right)_{ij} = fub, \qquad \left(n_{1_{\alpha\zeta}}\right)_{ij} = fus$$

$$\left(n_{1_{\beta\gamma}}\right)_{ij} = fvb, \qquad \left(n_{1_{\beta\zeta}}\right)_{ij} = fvs$$

$$\left(n_{1_{\gamma\gamma}}\right)_{ij} = fbb_1 - fbb_2 - (4/3h^2)fbb_3$$

$$\left(n_{1_{\gamma\zeta}}\right)_{ij} = fbb_1 - fbs_1 - fbs_3 - (4/3h^2)(fbs_2 + fbs_4)$$

$$\left(n_{1_{\zeta\zeta}}\right)_{ij} = fbb_1 - fss_2 - (4/3h^2)fss_3$$

$$\left(n_{2_{\gamma\gamma}}\right)_{ij} = \left(n_{2_{\gamma\zeta}}\right)_{ij} = \left(n_{2_{\zeta\zeta}}\right)_{ij} = \sum_{k=1}^{20}\sum_{l=1}^{20} w_k^b w_l^s$$
$$\times \{3A_{11}m_im_jm_km_l\Phi(m_{ijkl}-4, n_{ijkl})$$
$$+ 3A_{31}[(m_in_j + n_im_j)m_km_l + m_im_jm_kn_l]$$
$$\times \Phi(m_{ijkl}-3, n_{ijkl}-1)$$
$$+ (2A_{33} + A_{21})[(m_in_j + n_im_j)m_kn_l + n_in_jm_km_l$$
$$+ m_im_jn_kn_l]\Phi(m_{ijkl}-2, n_{ijkl}-2)$$
$$+ 3A_{32}[(m_in_j + m_jn_i)n_kn_l + n_in_jm_kn_l]$$
$$\times \Phi(m_{ijkl}-1, n_{ijkl}-3)$$
$$+ 3A_{22}n_in_jn_kn_l\Phi(m_{ijkl}, n_{ijkl}-4)$$
$$+ n_km_l[3A_{31}m_im_j\Phi(m_{ijkl}-3, n_{ijkl}-1)]$$
$$+ (2A_{33} + A_{2,1})(m_in_j + n_im_j)\Phi(m_{ijkl}-2, n_{ijkl}-2)$$
$$+ 3A_{32}n_in_j\Phi(m_{ijkl}-1, n_{ijkl}-3)]\}$$

in which

$$m_{ij} = m_i + m_j, \qquad n_{ij} = n_i + n_j$$

$$m_{ijk} = m_i + m_j + m_k, \qquad n_{ijk} = n_i + n_j + n_k$$

$$m_{ijkl} = m_i + m_j + m_k + m_l, \qquad n_{ijkl} = n_i + n_j + n_k + n_l$$

$$\Phi(m,n) = \int\int \xi^m \eta^n \, d\xi \, d\eta = c^{n+1}(a^{m+1} - b^{m+1})\frac{m!n!}{(m+n+2)!}$$

$$s_1 = m_k(m_k-1)m_im_j\Phi(m_{ijk}-4, n_{ijk})$$
$$s_2 = m_k(m_k-1)n_in_j\Phi(m_{ijk}-2, n_{ijk}-2)$$
$$s_3 = m_k(m_k-1)(m_in_j + n_im_j)\Phi(m_{ijk}-3, n_{ijk}-1)$$
$$s_4 = n_k(n_k-1)m_im_j\Phi(m_{ijk}-2, n_{ijk}-2)$$
$$s_5 = n_k(n_k-1)n_in_j\Phi(m_{ijk}, n_{ijk}-4)$$
$$s_6 = n_k(n_k-1)(m_in_j + n_im_j)\Phi(m_{ijk}-1, n_{ijk}-3)$$
$$s_7 = 2m_kn_km_im_j\Phi(m_{ijk}-3, n_{ijk}-1)$$
$$s_8 = 2m_kn_kn_in_j\Phi(m_{ijk}-1, n_{ijk}-3)$$
$$s_9 = 2m_kn_k(m_in_j + m_jn_j)\Phi(m_{ijk}-2, n_{ijk}-2)$$
$$t_1 = m_km_im_j(m_i + m_j - 2)\Phi(m_{ijk}-4, n_{ijk})$$
$$t_2 = n_k[m_i(m_i-1)n_j + n_im_j(m_j-1)]\Phi(m_{ijk}-2, n_{ijk}-2)$$
$$t_3 = \{m_k[m_i(m_i-1)n_j + n_im_j(m_j-1)]$$
$$+ n_km_im_j(m_im_j - 2)\}\Phi(m_{ijk}-3, n_{ijk}-1)$$
$$t_4 = m_k[n_i(n_i-1)m_j + m_in_j(n_j-1)]\Phi(m_{ijk}-2, n_{ijk}-2)$$
$$t_5 = n_kn_in_j(n_i + n_j - 2)\Phi(m_{ijk}, n_{ijk}-4)$$
$$t_6 = \{m_kn_in_j(n_i + n_j - 2) + n_k[n_i(n_i-1)m_j$$
$$+ n_j(n_j-1)m_i]\}\Phi(m_{ijk}-1, n_{ijk}-3)$$
$$t_7 = 2m_km_im_j(n_i + n_j)\Phi(m_{ijk}-3, n_{ijk}-1)$$
$$t_8 = 2n_kn_in_j(m_i + m_j)\Phi(m_{ijk}-1, n_{ijk}-3)$$
$$t_9 = 2[n_km_im_j(n_i + n_j) + m_kn_in_j(m_i + m_j)]$$
$$\times \Phi(m_{ijk}-2, n_{ijk}-2)$$
$$fub = fus = \sum_{k=1}^{20}\left(w_k^b + w_k^s\right)$$
$$\times \{A_{11}m_km_im_j\Phi(m_{ijk}-3, n_{ijk})$$
$$+ A_{31}[m_k(m_in_j + n_im_j) + n_km_im_j]\Phi(m_{ijk}-2, n_{ijk}-1)$$
$$+ A_{33}m_kn_in_j\Phi(m_{ijk}-1, n_{ijk}-2) + A_{23}n_kn_in_j$$
$$\times \Phi(m_{ijk}, n_{ijk}-3) + (A_{21}n_km_in_j + A_{33}n_kn_im_j)$$
$$\times \Phi(m_{ijk}-1, n_{ijk}-2)\}$$
$$fvb = fvb = \sum_{k=1}^{20}\left(w_k^b + w_k^s\right)$$
$$\times \{A_{13}m_km_im_j\Phi(m_{ijk}-3, n_{ijk})$$
$$+ A_{32}[n_k(m_in_j + n_im_j) + m_kn_in_j]\Phi(m_{ijk}-1, n_{ijk}-2)$$
$$+ A_{33}n_km_im_j\Phi(m_{ijk}-2, n_{ijk}-1) + A_{22}n_kn_in_j$$
$$\times \Phi(m_{ijk}, n_{ijk}-3) + (A_{12}m_kn_im_j + A_{33}m_km_in_j)$$
$$\times \Phi(m_{ijk}-2, n_{ijk}-1)\}$$
$$fbs_1 = fss_2 = \sum_{k=1}^{20} w_k^b(B_{11}s_1 + B_{21}s_2 + B_{31}s_3 + B_{12}s_4 + B_{22}s_5$$
$$+ B_{32}s_6 + B_{13}s_7 + B_{23}s_8 + B_{33}s_9)$$
$$fbs_2 = fbb_3 = \sum_{k=1}^{20} w_k^s(E_{11}s_1 + E_{21}s_2 + E_{31}s_3 + E_{12}s_4 + E_{22}s_5$$
$$+ E_{32}s_6 + E_{13}s_7 + E_{23}s_8 + E_{33}s_9)$$

$$fbb_1 = \sum_{k=1}^{20} u_k[A_{11}m_k m_i m_j \Phi(m_{ijk}-3, n_{ijk})$$
$$+ A_{21}m_k n_i n_j \Phi(m_{ijk}-1, n_{ijk}-2)$$
$$+ A_{31}m_k(m_i n_j + n_i m_j)$$
$$\times \Phi(m_{ijk}-2, n_{ijk}-1) + A_{13}n_k m_i m_j$$
$$\times \Phi(m_{ijk}-2, n_{ijk}-1) + A_{23}n_k n_i n_j \Phi(m_{ijk}, n_{ijk}-3)$$
$$+ A_{33}n_k(m_i n_j + n_i m_j)\Phi(m_{ijk}-1, n_{ijk}-2)]$$
$$+ \sum_{k=1}^{20} v_k[A_{12}n_k m_i m_j \Phi(m_{ijk}-2, n_{ijk}-1)$$
$$+ A_{22}n_k n_i n_j \Phi(m_{ijk}, n_{ijk}-3)$$
$$+ A_{32}n_k(m_i n_j + n_i m_j)$$
$$\times \Phi(m_{ijk}-1, n_{ijk}-2)$$
$$+ A_{13}m_k m_i m_j \Phi(m_{ijk}-3, n_{ijk}) + A_{23}m_k n_i n_j$$
$$\times \Phi(m_{ijk}-1, n_{ijk}-2)$$
$$+ A_{33}m_k(m_i n_j + n_i m_j)\Phi(m_{ijk}-2, n_{ijk}-1)]$$

$$fbb_2 = fbs_1 + \sum_{k=1}^{20}\left(w_k^b + w_k^s\right)(B_{11}t_1 + B_{21}t_2 + B_{31}t_3$$
$$+ B_{12}t_4 + B_{22}t_5 + B_{32}t_6 + B_{13}t_7 + B_{23}t_8 + B_{33}t_9)$$

$$fss_3 = fbs_2 + \sum_{k=1}^{20}\left(w_k^b + w_k^s\right)(E_{11}t_1 + E_{21}t_2 + E_{31}t_3$$
$$+ E_{12}t_4 + E_{22}t_5 + E_{32}t_6 + E_{13}t_7 + E_{23}t_8 + E_{33}t_9)$$

$$fbs_3 = \sum_{k=1}^{20}\left(w_k^b + w_k^s\right)$$
$$\times \{B_{11}m_k m_i(m_i-1)m_j \Phi(m_{ijk}-4, n_{ijk})$$
$$+ B_{21}n_k m_i(m_i-1)n_j \Phi(m_{ijk}-2, n_{ijk}-2)$$
$$+ B_{31}[m_k m_i(m_i-1)n_j + n_k m_i(m_i-1)m_j]$$
$$\times \Phi(m_{ijk}-3, n_{ijk}-1) + B_{12}m_k n_i(n_i-1)m_j$$
$$\times \Phi(m_{ijk}-2, n_{ijk}-2) + B_{22}n_k n_i(n_i-1)n_j$$
$$\times \Phi(m_{ijk}, n_{ijk}-4) + B_{32}[m_k n_i(n_i-1)n_j$$
$$+ n_k n_i(n_i-1)m_j]\Phi(m_{ijk}-1, n_{ijk}-3)$$
$$+ 2B_{13}m_k m_i n_i m_j \Phi(m_{ijk}-3, n_{ijk}-1)$$
$$+ 2B_{23}n_k m_i n_i n_j \Phi(m_{ijk}-1, n_{ijk}-3)$$
$$+ 2B_{33}(m_k n_j + n_k m_j)m_i n_i \Phi(m_{ijk}-2, n_{ijk}-2)\}$$

$$fbs_4 = \sum_{k=1}^{20}\left(w_k^b + w_k^s\right)$$
$$\times \{E_{11}m_k m_i m_j(m_j-1)\Phi(m_{ijk}-4, n_{ijk})$$
$$+ E_{21}n_k n_i m_j(m_j-1)\Phi(m_{ijk}-2, n_{ijk}-2)$$
$$+ E_{31}[m_k n_i m_j(m_j-1) + n_k m_i m_j(m_j-1)]$$
$$\times \Phi(m_{ijk}-3, n_{ijk}-1) + E_{12}m_k m_i n_j(n_j-1)$$
$$\times \Phi(m_{ijk}-2, n_{ijk}-2) + E_{22}n_k n_i n_j(n_j-1)$$
$$\times \Phi(m_{ijk}, n_{ijk}-4) + E_{32}[m_k n_i n_j(n_j-1)$$
$$+ n_k m_i n_j(n_j-1)]\Phi(m_{ijk}-1, n_{ijk}-3)$$
$$+ 2E_{13}m_k m_i m_j n_j \Phi(m_{ijk}-3, n_{ijk}-1)$$
$$+ 2E_{23}n_k n_i m_j n_j \Phi(m_{ijk}-1, n_{ijk}-3)$$
$$+ 2E_{33}(m_k n_i + n_k m_i)m_j n_j \Phi(m_{ijk}-2, n_{ijk}-2)\}$$

References

[1]Stein, M., "The Phenomenon of Change in Buckle Pattern in Elastic Structures," NASA TR R-39, 1959.

[2]Stein, M., "Loads and Deformations of Buckled Rectangular Plates," NASA TR R-40, 1959.

[3]Yamaki, N., "Postbuckling Behavior of Rectangular Plates with Small Initial Curvature Loaded in Edge Compression," *Journal of Applied Mechanics*, Vol. 26, No. 3, 1959, pp. 407–414.

[4]Rushton, K. R., "Post-buckling of Rectangular Plates with Various Boundary Conditions," *Aeronautical Quarterly*, Vol. 21, May 1970, pp. 163–181.

[5]Stein, M., "Postbuckling of Orthotropic Composite Plates Loaded in Compression," *AIAA Journal*, Vol. 21, No. 12, 1983, pp. 1729–1735.

[6]Jensen, D. W., and Lagace, P. A., "Influence of Mechanical Coupling on the Buckling and Postbuckling of Anisotropic Plates," *AIAA Journal*, Vol. 26, No. 10, 1988, pp. 1269–1277.

[7]Minguet, P. J., Dugundji, J., and Lagace, P., "Postbuckling Behavior of Laminated Plates Using a Direct Energy-Minimization Technique," *AIAA Journal*, Vol. 27, No. 12, 1989, pp. 1785–1792.

[8]Dawe, D. J., and Lam, S. S. E., "Non-linear Finite Strip Analysis of Rectangular Laminates Under End Shortening Using Classical Plate Theory," *International Journal for Numerical Methods in Engineering*, Vol. 35, No. 5, 1992, pp. 1087–1110.

[9]Lam, S. S. E., and Dawe, D. J., "Non-linear Finite Strip Analysis of Rectangular Laminates Under End Shortening Using Shear Deformation Plate Theory," *International Journal for Numerical Methods in Engineering*, Vol. 36, No. 6, 1993, pp. 1045–1064.

[10]Chia, C. Y., "Geometrically Nonlinear Behavior of Composite Plates: A Review," *Journal of Applied Mechanics Review*, Vol. 41, No. 12, 1988, pp. 439–451.

[11]Shin, D. K., Griffin, O. H., Jr., and Gurdal, Z., "Postbuckling Response of Laminated Plates Under Uniaxial Compression," *International Journal Non-linear Mechanics*, Vol. 28, No. 1, 1993, pp. 95–115.

[12]Shiau, L. C., and Wu, T. Y., "A High Precision Higher Order Triangular Element for Free Vibration of General Laminated Plates," *Journal of Sound and Vibration*, Vol. 161, No. 2, 1993, pp. 265–279.

[13]Jones, R. M., *Mechanics of Composite Material*, Scripta, Washington, DC, 1975, pp. 152–155.

[14]Yang, T. Y., *Finite Element Structural Analysis*, Prentice–Hall, Englewood Cliffs, NJ, 1986, pp. 450–455.

[15]Chia, C. Y., *Nonlinear Analysis of Plates*, McGraw–Hill, New York, 1980, Chap. 8.